

Synthesis, Characterisation and Catalytic Performance of Porous Nafion Resin/Silica Nanocomposites for Esterification of Lauric Acid and Methanol

H. N. Lim^{1*}, M. A. Yarmo¹, N. M. Huang², P. S. Khiew³ and W. S. Chiu³

¹School of Chemical Sciences and Food Technology, Faculty of Science and Technology, Universiti Kebangsaan Malaysia, 43600 Bandar Baru Bangi, Selangor, Malaysia.

²Solid State Physics Research Group, Physics Department, Faculty of Science, Universiti Malaya, 50603 Kuala Lumpur, Malaysia.

³Faculty of Engineering and Computer Science, Nottingham University, Jalan Broga, 43500 Semenyih, Selangor Darul Ehsan, Malaysia.

*Corresponding author: janet_limhn@yahoo.com

Abstract: *Solid acid catalyst nanocomposites made from Nafion resin supported on silica were prepared using an in situ sol-gel technique. Nafion resin/silica nanocomposites combined the solid acid catalyst properties of Nafion resin with the high surface area characteristic of silica as a porous support. Nitrogen gas adsorption-desorption showed that the surface area of Nafion resin supported on silica increased by about 10,000 times compared to the surface area of pure Nafion resin (0.02 m²/g). The use of Nafion resin/silica nanocomposites as catalysts for the esterification of lauric acid and methanol increased the methyl laurate yield by three fold compared to pure Nafion resin.*

Keywords: nanocomposite, catalyst, sol-gel, esterification, Nafion resin

Abstrak: *Mungkin nanokomposit asid pepejal berdasarkan resin Nafion disokong pada silika disediakan melalui teknik sol-gel in situ. Nanokomposit resin Nafion/silika menggabungkan sifat-sifat mungkin asid pepejal resin Nafion dengan ciri luas permukaan tinggi silika sebagai penyokong porous. Penjerapan-penyahjerapan gas nitrogen menunjukkan bahawa luas permukaan resin Nafion yang disokong pada silika meningkat sebanyak 10 000 kali berbanding dengan luas permukaan resin nafion tulen (0.02 m²/g). Penggunaan nanokomposit resin Nafion sebagai mungkin untuk esterifikasi asid laurik dan metanol menambahkan hasil metil laurat sebanyak tiga kali ganda berbanding dengan resin Nafion tulen.*

Kata kunci: nanokomposit, mungkin, sol-gel, esterifikasi, resin Nafion

1. INTRODUCTION

Esterification is a very important reaction in the synthesis of many organic substances of great interest in the field of fine chemistry.¹ Esterification is usually catalysed by an acid catalyst proton donor, like sulphuric or sulphonic acid.² The conventional esterification process, which employs those acids, can

result in sulphur contamination of the final ester product. This also has the effect of poisoning catalysts that are used downstream. The use of homogeneous acids also requires neutralisation with alkali. In general, the process efficiency is less than 96%, and the neutralisation step creates a waste disposal problem.³

There is now increasing interest in finding new alternative solid acid catalysts for esterification that would eliminate final ester contamination and minimise effluent problems.³ Nafion resin is quickly gaining popularity for use in esterification reactions.^{4,5} Nafion resin, which is perfluorinated sulphuric acid, has an acid strength equivalent to that of concentrated sulphuric acid. Nafion resin was developed about thirty years ago and is known to catalyse a wide variety of reactions.^{6,7} Nafion resin exhibits superacidity due to the electron-withdrawing effect of the perfluorocarbon chain on the pendant sulphonic acid group (Fig. 1).

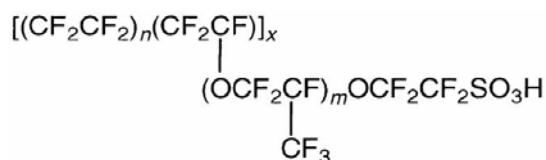


Figure 1: General structure of Nafion resin; $m = 1, 2$ or 3 ; $n = 6, 7$; $x = \sim 100$.

However, one major disadvantage of commercially available Nafion resin beads is their very low surface area ($0.02 \text{ m}^2\text{g}^{-1}$), which limits the utility of these materials because most of the active sites are buried within the polymer beads. Under many types of reaction conditions, these sites are inaccessible or poorly accessible, and as a result, the observed activity for many reactions is very low.⁸

In order to increase the acid site accessibility of Nafion resin, this material is supported on high surface area oxides that enhance catalytic performance. Researchers at DuPont reported the preparation of a novel high surface area Nafion resin/silica nanocomposite catalyst in which Nafion particles are encapsulated within a porous silica network.⁸ The effective surface area of the resin increased significantly as the resin particles were entrapped within the highly porous silica network. Therefore, a higher number of acid sites were exposed, which in general provides enhanced catalytic effects. Nafion resin/silica nanocomposites have been utilised in various kinds of reactions, including olefin isomerisation, but-1-ene isomerisation,⁹ Friedel-Crafts benzylation,^{10,11} dimerisation, esterification,¹² acylation^{13,14} and epoxidation.¹⁵

In this paper, we report using Nafion resin/silica nanocomposites as catalysts for the esterification of lauric acid and methanol to yield methyl laurate for the first time. Nafion resin/silica nanocomposites were synthesised via an *in situ* sol-gel technique prior to testing the catalytic performance of the nanocomposites by varying parameters such as the amount of Nafion resin loaded on the silica support, temperature, molar ratio and hydrocarbon chain length. The influences of these parameters on catalytic performance are discussed in detail.

2. EXPERIMENTAL

2.1 Synthesis of Nafion Resin/Silica

Tetraethylorthosilicate (TEOS, $\text{Si}(\text{EtO})_4$, 99%) was obtained from Fluka and used as received. The Nafion resin perfluorinated ion-exchange polymer was a 5 wt% solution that was prepared under pressure in a mixed water-alcohol system. Nafion resin solutions are available from Aldrich. A two-step acid/base hydrolysis and condensation of alkoxy silane was used in this synthesis. In a typical synthesis procedure, a mixture of 7.93 g TEOS, 2 ml deionised water and 0.5 ml 0.04 M HCl was stirred until a clear solution was obtained. Nafion resin solution (2.5 ml) was added to the clear silicon solution while stirring. Later, 0.4 M NaOH solution was added until the mixture gelled to form a hard, solid mass that was slightly opaque. The solid gel was placed in an oven and dried at about 95°C over a period of about 2 days, followed by drying under vacuum overnight at 95°C. Then, the product was gently ground into powder. The resulting composite was reacidified by stirring with 40 ml of 3.5 M HCl aqueous solution and washed with deionised water. This process was repeated five times. Finally, the product was dried under vacuum at 95°C for 24 h. Six different Nafion resin composites (containing 5, 13, 20, 40 and 60 wt% Nafion resin) were prepared by varying the weights and ratio of the Nafion resin and TEOS. Hereafter, the nanocomposites were labelled as NR/S-X, where X refers to the Nafion resin load used in the synthesis.

2.2 Characterisation

The surface area of the NR/S nanocomposites was determined using a nitrogen gas adsorption technique at 77 K. Before the measurement of nitrogen adsorption-desorption, each sample was dried in an oven at 95°C overnight to avoid adsorption of vapour in the nanocomposite pores. The surface area of a specific region was determined by taking into account the linear portion in the BET plot. The resulting nanocomposite materials were observed under a Meiji optical microscope and further investigated using a LEO 120 energy-filtered transmission electron microscope (EFTEM) operating an acceleration voltage of

120 kV. For the electron microscope characterisation, a 1.0 wt% sample was dispersed in an ethanol solution. A drop of the solution was cast on a carbon-coated copper grid (400 mesh, Agar Scientific) and allowed to evaporate at room temperature before observation under an electron microscope. The surfaces of the nanocomposites were observed using an Oxford Instrument model 7353 scanning electron microscope (SEM) with a 138 eV resolution. Before the sample was observed under the SEM, the sample was positioned atop an aluminium stub using double-sided tape and sputtered with gold. Fourier transform infrared spectroscopy (FTIR) was carried out using a Perkin Elmer instrument. Sample preparation was based on the KBr technique, and the powder was mixed with potassium bromate, ground homogeneously and converted into pellet form.

2.3 Catalytic Performance

The reagents used for catalytic tests were methanol (J.T. Baker, 100%) and lauric acid (POFAC 1299). Esterification reactions between lauric acid and methanol were carried out in a stirred, three-neck, round-bottom flask under atmospheric pressure heated by an Electromantle MA solid state stirrer. The flask was connected to a condenser so that any vapours given off were cooled back into liquid and fell back into the reaction vessel, following a reflux mechanism. Reaction temperatures were controlled to $\pm 1^\circ\text{C}$ using a thermometer immersed in the reactants mixture. The reaction parameters studied were the Nafion resin load supported on the silica, temperature, molar ratio of methanol to lauric acid and hydrocarbon length. The samples were collected for 24 h. Experiments with no catalyst were carried out in order to evaluate the extension of the homogeneous reaction.

2.4 Identification and Analysis of Reaction Products

The reaction products were diluted with heptane and analysed using a Hewlett Packard Type 6890 flame ionization detector (FID) gas chromatograph (GC). The products were separated using a fused silica capillary column with a 30 m length, a 0.32 mm internal diameter and a 0.2 μm thickness, operated at T_{injector} and T_{detector} of 250°C . The column temperature program was set and the temperature was increased from 110°C to 160°C at 6°C min^{-1} , then from 160°C to 180°C at 4°C min^{-1} , then from 180°C to 210°C at $20^\circ\text{C min}^{-1}$, and the final temperature (250°C) was maintained for 15 min in order to remove any high boiling impurities. Lauric acid conversion as well as the selectivity and yield of methyl laurate were calculated based on GC chromatograms by taking into account an external standard of lauric acid and methyl laurate.

3. RESULTS AND DISCUSSION

In gas nitrogen adsorption-desorption for NR/S nanocomposites, capillary condensation occurs in the pores whereby p/p_0 (relative nitrogen pressure) is linked to pores that are filled by nitrogen gas.^{16,17} The adsorption-desorption isotherm for nanocomposites was isotherm type IV, which is the isotherm for mesoporous structured material (Fig. 2). Studies of mesoporous pore structure are always linked to isotherm type IV. One characteristic of isotherm type IV is the hysteresis loop. The shape of the hysteresis loop changes for different systems. However, one similar characteristic is that the adsorbed amount is always higher along desorption than adsorption at p/p_0 . Isotherm type IV is always found in xerogel oxidised inorganic material and porous structures. From isotherm type IV, it can be determined that the mesoporosity of the nanocomposites resulted from closely arranged spherical particles (Fig. 3).

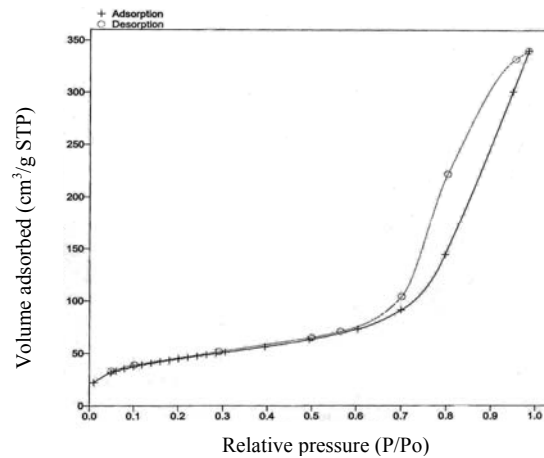


Figure 2: Nitrogen gas adsorption-desorption isotherm at 77 K for NR/S-13 nanocomposite.

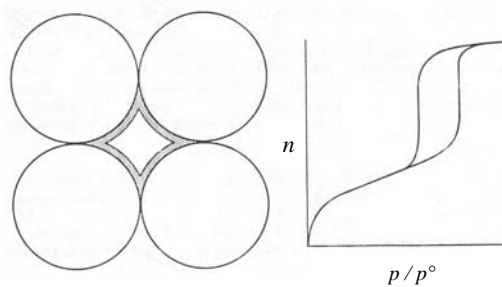


Figure 3: Pores formed from closely arranged spherical particles and the ideal isotherm for the pores.

Generally, the surface area of the nanocomposites decreased from 190 to $135 \text{ m}^2\text{g}^{-1}$ as the Nafion resin load increased. However, the NR/S-60 nanocomposite had a surface area that was far lower than the rest of the nanocomposites ($15.3 \text{ m}^2\text{g}^{-1}$). The NR/S-60 nanocomposite had the biggest pore size ($\sim 156 \text{ \AA}$), compared to NR/S-5, 13, 20 and 40 nanocomposites, which were in the range of $75\text{--}100 \text{ \AA}$ (Table 1). The pore size values are in accordance with the values reported in EFTEM.

Table 1: Surface area measured by the BET technique, external surface area and pore size of the NR/S nanocomposites.

Sample	Surface area (BET) (m^2g^{-1})	Pore size (\AA)
NR/S-5	189.4	111.8
NR/S-13	159.6	108.0
NR/S-20	173.9	86.3
NR/S-40	134.5	74.6
NR/S-60	15.3	156.5

Figure 4 is the EFTEM micrograph of the NR/S-13 nanocomposite, showing the particulate substructure and also the porosity, which is indicated by the white areas. The pore diameter is about 10 nm , which is in accordance with the BET results.

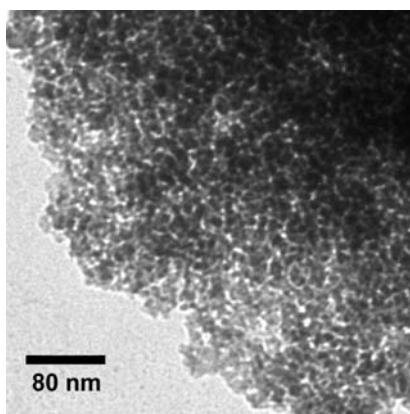
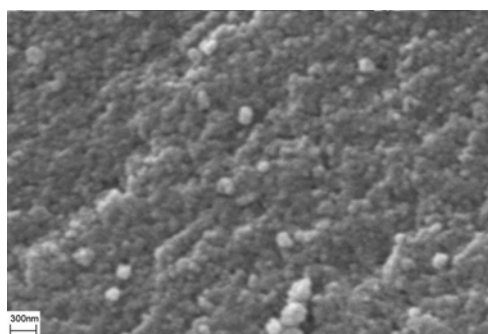
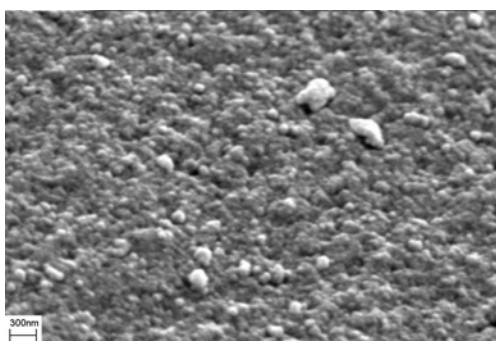


Figure 4: EFTEM micrograph of the NR/S-13 nanocomposite.

The SEM micrograph in Figure 5(a) shows the surface of the NR/S-13 nanocomposite. The microstructure is particulate in nature with primary particles in the range of 30 to 50 nm. Gelation occurred, following nucleation and growth of the primary particles via particle condensation and cross-linking to form the extended network. Figure 5(b) represents the calcined NR/S-13 nanocomposite at 600°C with the polymer completely removed. The presence of the voids is apparent, with diameters in the range of 40 to 70 nm. The silicate matrix undergoes very little microstructural change (except for the loss of silanols) at 600°C, and thus it is reasonable to assume that the created voids in the nanoparticles reflect the original dispersion of the Nafion resin. The higher the Nafion resin load, the larger the pore size, apart from NR/S-60. Elemental mapping by SEM confirmed that the Nafion resin was well dispersed in the silica medium.



(a)



(b)

Figure 5: Uncalcined (a) and calcined (b) NR/S-13 nanocomposite at 600°C.

Figure 6 shows the FTIR spectra of NR/S-5, 13, 20, 40 and 60. All the nanocomposite spectra exhibited similar peaks at 470, 800, 950, 1110, 1650 and 3400 cm^{-1} . The S-O stretch was assigned to an absorption peak at 1050 cm^{-1} .

However, the S-O stretch was overlapped by a broad peak at 1110 cm^{-1} . The Si-O-Si bonds were confirmed by the absorption peaks at 470 , 800 and 1110 cm^{-1} , which were ascribed to bond bending vibration, symmetric bond stretching vibration and turnover from Si-O-Si asymmetric bond stretching vibration, respectively.¹⁸ The presence of Si-OH was confirmed by the peak at 955 cm^{-1} , which was associated with its stretching mode vibration. The peak at $1650\text{--}1600\text{ cm}^{-1}$ was due to the deformation from adsorbed molecular water, and the band at around 3400 cm^{-1} corresponded to structural hydroxyl groups and also OH stretching of physically absorbed water. There were two peaks at 1216 and 1148 cm^{-1} for the NR/S nanocomposites with the 40 and 60 wt% Nafion resin load, respectively, which were assigned to the C-F stretching modes. However, those two particular peaks for 5, 13 and 20 wt% samples were not well resolved due to broad overlap by the 1110 cm^{-1} peak.

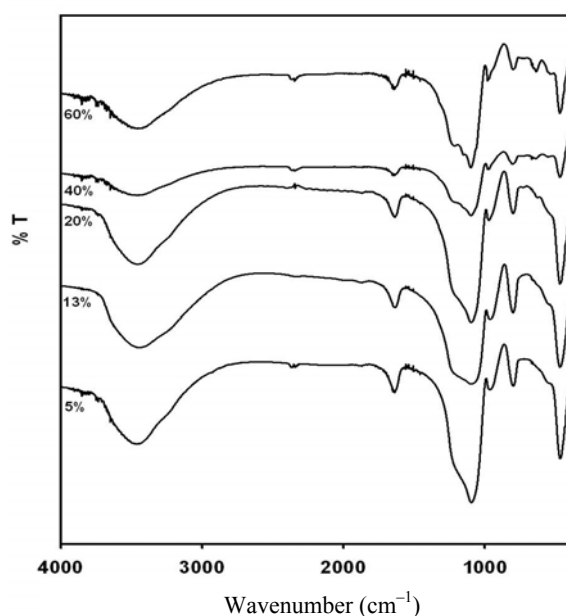
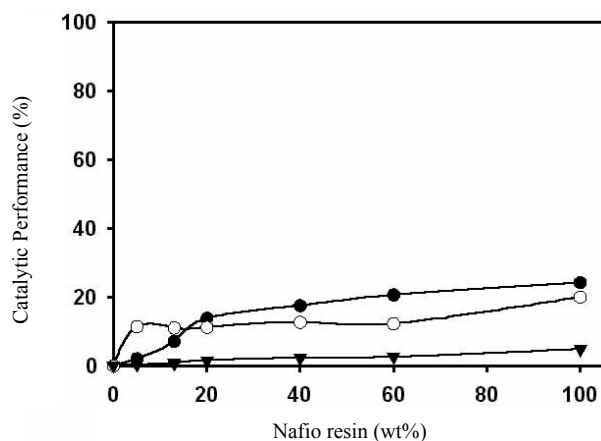


Figure 6: FTIR spectra for NR/S-5, 13, 20, 40 and 60 nanocomposites.

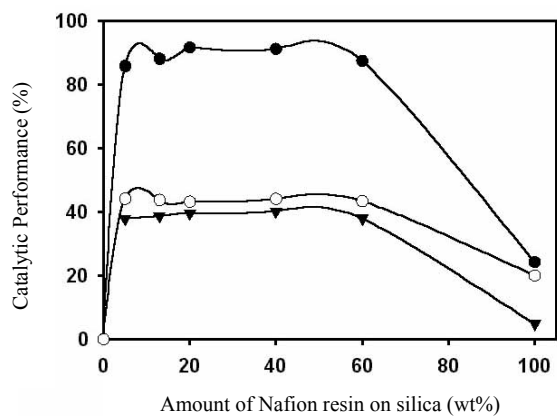
3.1 Influence of Nafion Resin Load

Figure 7(a) shows the catalytic activity of unsupported Nafion resin, and Figure 7(b) shows the catalytic activity of NR/S nanocomposites with various amounts of loaded Nafion resin. Unsupported Nafion resin was found to have much lower activity compared to that of the Nafion resin nanocomposites. Even though Nafion resin swelled in the presence of methanol due to the formation of

hydrogen bonds between the sulphonic groups of the resin and the alcohol molecules of the reaction mixture, the inner active sites within the resin could not be fully exposed. This decreased lauric acid diffusion and limits the accessibility of reactants to the active sites located in the pores of the polymer structure, which became the limited step of the esterification.¹⁹ This problem was circumvented by designing a catalyst where the majority of the acid sites were accessible on the surface to both the acid and alcohol, yielding a very rapid esterification reaction with negligible amounts of etherification.³



(a)



(b)

Figure 7: Conversion (●), selectivity (○) and yield (▼) of methyl laurate from the esterification of lauric acid and methanol as a function of (a) Nafion resin and (b) Nafion resin load in the NR/S nanocomposite.

For NR/S nanocomposites, the conversion of lauric acid increased rapidly before reaching a plateau at 20 wt%. The selectivity for methyl laurate was constant until 40 wt% of Nafion resin was loaded, whereas the yield for methyl laurate increased steadily until 40 wt% Nafion resin. NR/S-20 nanocomposite showed catalytic activity comparable to that of NR/S-40 nanocomposite. This showed that higher concentrations of surface groups did not necessarily lead to higher conversions; in fact, good access to the active sites seems to be more important.²⁰ The catalytic performance decreased at a 60 wt% load and higher. This is possibly because the continuity of the porous silica network was disrupted as the polymer microstructure started to dominate the pore characteristics at higher polymer loads. Catalyst activity for 100 wt% Nafion resin was much lower than that of NR/S nanocomposite with a Nafion resin load of 5 wt%, as shown in Table 2.

Table 2: Comparison of the effects of NR/S-5 nanocomposite and Nafion resin on the esterification reaction.

Type of catalyst	Conversion (%)	Selectivity (%)	Yield (%)
Blank	14.2	12.0	1.7
NR/S-5 nanocomposite	85.8	44.1	37.9
Nafion resin	24.2	20	4.8

Experimental conditions: molar ratio (lauric acid:methanol) = 1:4, T = 75°C and time = 24 h.

These results clearly show the enhanced accessibility of the acid sites in the composite structure, where Nafion resin was well distributed on the surface of the silica. Additionally, the surface area of the nanocomposite increased, and thus the number of acid sites also increased. Machado et al.²¹ reported that a high yield of product can be attributed to a transition state shape selectivity that encourages the esterification to methyl laurate. The NR/S-20 nanocomposite showed higher selectivity to methyl laurate than the Nafion resin. This behaviour may be due to the fact that active sites are only available on the external surface of Nafion resin, which has no shape selectivity and can form other derivatives besides methyl laurate. Therefore, for Nafion resin, the reaction takes place mainly at the external surface of the resin where shape selectivity does not exist.¹⁶ On the other hand, the reaction might occur on the internal sites of the NR/S-20 structure and therefore control the shape selectivity of the product.

3.2 Reaction Temperature

The reaction at 75°C gave the best catalytic activities (Table 3), as the temperature allowed the reactant molecules to gain enough energy (heat) to diffuse into the pores. Moreover, side reactions such as dehydration, polymerisation and acid decomposition were inhibited when the esterification

was accomplished at a relatively low temperature (75°C). However, the catalytic reaction diminished at 85°C compared to 105°C. It was expected that at relatively high temperatures, Nafion resin would leach from the silica support. This was supported by the elemental mapping analysis. Nevertheless, Beers et al.²² reported that decomposition of Nafion resin does not happen through the leaching test. Moreover, methanol is not stable at relatively high temperatures, and thus evaporation of the alcohol occurred during the esterification reaction and may have reduced any interaction between the lauric acid and methanol. At 65°C, the catalytic performance was at its lowest due to the immiscibility of the reactants, which diminished the surface contact and disfavoured the reaction.²⁰

Table 3: Influence of temperature on the esterification reaction.

Temperature (°C)	Conversion (%)	Selectivity (%)	Yield (%)
(75 blank)	14.2	12.0	1.7
65	73.2	34.8	25.4
75	91.6	43.2	39.6
85	87.4	40.1	35.1
95	76.9	38.5	29.6
105	74.5	37.4	27.9

Experimental conditions: molar ratio (lauric acid:methanol) = 1:4, catalyst amount = 0.8 wt% NR/S-20 nanocomposite, and time = 24 h.

The selectivity of nanocomposites for all temperatures was higher than that of the blank due to the shape selectivity effect of methyl laurate in the pores. Shape constriction in the pores limits any secondary reactions that may form side products in the pores. In the blank reaction, the secondary reactions were not limited and thus lowered the reaction selectivity to methyl laurate.²³

3.3 Influence of the Molar Ratio of Methanol to Lauric Acid, R

It was found that both the lauric acid conversion and selectivity to methyl laurate increased when R increased (Table 4). A plausible explanation is that when the molar ratio increased, lauric acid had a better chance of reacting with methanol, and thus the selectivity to methyl laurate increased due to the forward-shifting of the reversible reaction. As predicted, an increment in selectivity was observed when R increased from 1 to 4. This observation is in agreement with Bossaert et al.²⁰

Table 4: Influence of the molar ratio of methanol:lauric acid, R , on the esterification reaction.

Molar ratio of methanol:lauric acid, R	Conversion (%)	Selectivity (%)	Yield (%)
0.5	32.7	30.9	10.1
1	41.6	32.4	13.5
2	66.8	34.6	23.1
4	91.6	43.2	39.6

Experimental conditions: $T = 75^{\circ}\text{C}$, catalyst amount = 0.8 wt% NR/S-20 nanocomposite and time = 24 h.

Maximum acid conversion at $R = 4$ can be explained by the critical need of methanol to expand the resin matrix and the solvation of sulphonic groups for the esterification reaction. For $R < 4$, a small amount of methanol was being used for partial expansion of the resin and thus, acid conversion was low. There was a significant increase in conversion when the amount of methanol increased. This result could mean that for a low value of R , the reaction occurs only at the surface of the resin particle, while by increasing the value of R to 4, the esterification reaction might occur over the sites in the pores.¹⁹

3.4 Influence of the Hydrocarbon Chain Length on the Acid

The influence of the hydrocarbon chain length on the diffusion rate of the acid in the catalyst was studied. The results present in Table 5 clearly showed that the nature of the acid greatly influenced the activity of the catalyst. The esterification reaction was more rapid with lauric acid (C_{12}) than with stearic acid (C_{18}). It is suggested that the diffusion of lauric acid was easier with the gel phase of the resin in the catalyst due to the chain length effect and its facilitation of adsorption on the strong protonic sites. Therefore, the adsorption and diffusion of the ester outside the catalyst were also more rapid.¹⁹

Table 5: Influence of hydrocarbon chain length on the esterification reaction.

Fatty acid	Conversion (%)	Selectivity (%)	Yield (%)
Lauric	91.6	43.2	39.6
Stearic	48.9	22.0	10.8

Experimental conditions: molar ratio (lauric acid:methanol) = 1:4, $T = 75^{\circ}\text{C}$, catalyst amount = 0.8 wt% NR/S-20 nanocomposite and time = 24 h.

4. CONCLUSION

NR/S nanocomposites were successfully synthesised and utilised as catalysts for the esterification of lauric acid and methanol to produce methyl laurate for the first time. Observation by SEM proved that Nafion resin was

distributed evenly on the silica matrix. EFTEM further showed that the nanocomposites had a mesoporous structure with pore diameters of about 10 nm. This value was supported by nitrogen gas adsorption-desorption analysis that showed pore diameters in the range of 7–11 nm, depending on the Nafion resin load. The surface area of Nafion resin supported on silica increased up to 10,000 times. Fourier transform infrared spectroscopy (FTIR) did not exhibit new peaks, which implied the absence of chemical bonding between Nafion resin and silica.

NR/S nanocomposites were proven as potential catalysts in the esterification reaction between methanol and lauric acid. These catalysts were able to give satisfactory catalytic performance per catalyst mass compared to Nafion resin. This is due to the increase in surface area and accessibility of the acid sites in Nafion resin. The esterification reaction at 75°C and $R = 4$ gave rise to the best catalytic performance. An increase in hydrocarbon chain length decreased the catalytic performance due to decrease accessibility to the active sites in the pores because of steric hindrance. These nanocomposites were easily separated from the reaction compared to mineral acids. Diffusion limitation was overcome effectively by using a thin layer of Nafion resin on the silica support.

5. ACKNOWLEDGEMENTS

The authors wish to thank the Malaysian Ministry of Science and Technology for financial support through IRPA research grant 09-02-02-0033.

6. REFERENCES

1. Kirumakki, S. R., Nagaraju, N., Murthy, K. V. V. S. B. S. R. & Narayanan, S. (2002). *Appl. Catal. A.*, 226, 175.
2. Kale, V., Subbaras, R., Lakshminarayana, G. & Bhagwant Rao, M. (1994). *J. Am. Oil Chem. Soc.*, 9, 1035.
3. Harmer, M. A. & Sun, Q. (2001). *Appl. Catal. A.* 221, 45.
4. Waller, F. J. & Van Scayoc, R. W. (1987). *Chem. Tech.*, 438.
5. Olah, G. A., Iyer, P. S. & Prakash, G. K. S. (1986). *Synthesis*, 513.
6. Olah, G. A., Arvanaghi, M. & Krishnamurthy, V. V. (1983). *Org. Chem.*, 48, 3359.
7. Olah, G. A. (1994). In J. Fraissard and L. Fetrakis (Eds.), *Acidity and Basicity of Solids*. Netherlands: Kluwer, 305.
8. Harmer, M. A., Farneth, W. E. & Sun, Q. (1996). *J. Am. Chem. Soc.*, 118, 7708.
9. Sun, Q., Harmer, M. A. & Farneth, W. E. (1996). *Chem. Commun.*, 1201.

10. _____ (1997). *Ind. Eng. Chem. Res.*, 36, 5541.
11. Beltrame, P. & Zuretti, G. (2005). *Appl. Catal. A*, 283, 33.
12. Heidekum, A., Harmer, M.A. & Hoelderich, W.F. (1999). *J. Catalysis*, 188, 230.
13. Schuster, H. & Holderich, W.F. (2008). *Appl. Catal. A*, 350, 1.
14. Martinez, F., Morales, G., Martin, A. & van Grieken, R. (2008). *Appl. Catal. A*, 347, 169.
15. Schuster, H., Rios, L. A., Weckes, P. P. & Hoelderich, W. F. (2008). *Appl. Catal. A*, 348, 266.
16. Gregg, S. J. & Sing, K. S. (1982). *Adsorption surface area and porosity*, New York: Academic.
17. Barret, E. P., Jayner, L. G. & Halenda, P. P. (1951). *J. Am. Chem. Soc.*, 73, 373.
18. Wang, L., Wang, Z., Zhao, J., Yuan, Z., Yang, H. & Zhao, M. (1999). *Mater. Chem. Phys.*, 59, 171.
19. Pouilloux, Y., Abro, S., Vanhove, C. & Barrault, J. (1999). *J. Mol. Catal. A: Chem.*, 149, 243.
20. Bossaert, W. D., Vos, D. E. D., Rhijn, W. M. V., Bullen, J., Grobet, P. J. & Jacobs, P. A. (1999). *J. Catal*, 182, 156.
21. Machado, M. S., Perez-Pariente, J., Sastre, E., Cardoso, D. & de Guereñu A. M. (2000). *Appl. Catal. A*, 203, 321.
22. Beers, A. E. W., Nijhuis, T. A. & Kapteijn, F. (2001). In R. A. Sheldon & H. van Bekkum (Eds.), *Solid-acid Catalyst-General (pp116)*., Weinheim: Wiley-VCH.
23. Diaz, I., Mohino, F., Perez-Pariente, J. & Sastre, E. (2001). *Appl. Catal. A Gen.*, 205, 19.